Flavin, M., & Murofushi, H. (1984) *Methods Enzymol. 106*, 223-237.
Folk, J. E. (1971) In *The Enzymes* (Boyer, P. D., Ed.) Vol. III, pp 57-79, Academic Press, New York.
Frickler, L. D., & Snyder, S. H. (1983) *J. Biol. Chem. 258*, 10950-10955.
Greene, L. A., & Tischler, A. S. (1976) *Proc. Natl. Acad. Sci. U.S.A. 73*, 2424-2428.
Gundersen, G. G., & Bulinski, J. C. (1988) *Proc. Natl. Acad. Sci. U.S.A. 85*, 5946-5950.
Gundersen, G. G., Kalnoski, M. H. & Bulinski, J. C. (1984) *Cell 38*, 779-789.
Gundersen, G. G., Khawaja, S., & Bulinski, J. C. (1987) *J. Cell. Biol. 105*, 251-264.
Gundersen, G. G., Khawaja, S., & Bulinski, J. C. (1989) *J. Cell. Biol. 109*, 2275-2288.
Hallak, M. E., Rodriguez, J. A., Barra, H. S., & Caputto, R. (1977) *FEBS Lett. 73*, 147-150.
Hecht, N. B., Distel, R. J., Yelick, P. C., Tanhauser, S. M., Driscoll, C. E., Golberg, E., & Tung, K. S. K. (1988) *Mol. Cell. Biol. 8*, 996-1000.
Johnson, K. A., & Borisy, G. G. (1977) *J. Mol. Biol. 117*, 1-31.
Kirschke, H., & Barrett, A. J. (1987) in *Lysosomes: Their role in protein breakdown* (Glaumann, H., & Ballard, F. J., Eds.) pp 193-238, Academic Press, London.
Kumar, N., & Flavin, M. (1981) *J. Biol. Chem. 256*, 7678-7686.
Laemmli, U. K. (1970) *Nature 227*, 680-685.
Lim, S.-S., Sammak, P. J., & Borisy, G. G. (1989) *J. Cell Biol. 109*, 253-264.
Matsuda, K., & Misaka, E. (1975) *J. Biochem. 78*, 31-39.
Murofushi, H. (1980) *J. Biochem. 87*, 979-984.
Paturle, L., Wehland, J., Margolis, R. L., & Job, D. (1989) *Biochemistry 28*, 2698-2704.
Pratt, L. F., Okamura, S., & Cleveland, D. (1987) *Mol. Cell. Biol. 7*, 552-555.
Raybin, D., & Flavin, M. (1977) *Biochemistry 16*, 2189-2194.
Rodriguez, J. A., Arce, C. A., Barra, H. S., & Caputto, R. (1973) *Biochem. Biophys. Res. Commun. 54*, 335-340.
Ryan, C. A., Hass, G. M., Kuhn, R. W., & Neurath, H. (1974) in *Proteinase Inhibitors* (Fritz, H., Tschesche, H., Greene, L. J., & Truscheit, E., Eds.) pp 565-573, Springer-Verlag, New York.
Schroder, H. C., Wehland, J., & Weber, K. (1985) *J. Cell Biol. 100*, 276-281.
Sullivan, K. (1988) *Annu. Rev. Cell Biol. 4*, 687-716.
Towbin, H., Staehelin, T., & Gordon, J. (1979) *Proc. Natl. Acad. Sci. U.S.A. 76*, 4350-4354.
Vallee, R. (1986) *Methods Enzymol. 134*, 89-104.
Webster, D. R., Gundersen, G. G., Bulinski, J. C., & Borisy, G. G. (1987) *J. Cell Biol. 105*, 265-276.
Webster, D. R., Wehland, J., Weber, K., & Borisy, G. G. (1990) *J. Cell Biol. 111*, 113-122.
Wehland, J., & Weber, K. (1987a) *J. Cell Sci. 88*, 185-203.
Wehland, J., & Weber, K. (1987b) *J. Cell Biol. 104*, 1059-1067.

Cutoff Size Does Strongly Influence Molecular Dynamics Results on Solvated Polypeptides†

H. Schreiber and O. Steinhauser*

Molecular Dynamics Group, Institute for Theoretical Chemistry, Währingerstrasse 17, A-1090 Vienna, Austria

Received November 6, 1991; Revised Manuscript Received February 12, 1992

ABSTRACT: The behavior of a 17-residue model peptide is analyzed by means of molecular dynamics simulations including explicitly more than a thousand water molecules. On the basis of the charge-group concept, Coulomb interactions are truncated for three values of the cutoff radius: 0.6, 1.0, and 1.4 nm. It is found that the stability of an α-helix, which acts as a common starting configuration, is a function of the cutoff size. While the overall stability of the helix is conserved in a simulation using a cutoff of 1.0 nm, it is lost within a very short period of 100 ps when the cutoff is increased to 1.4 nm. This demonstrates that the commonly used cutoff size of 1.0 nm is inappropriate because it does not ensure the convergence of Coulomb interactions. In order to permit an independent judgment, we have performed a 225-ps simulation using the Ewald summation technique, which is more elaborate but circumvents the problem to find an appropriate cutoff value. In contrast to the 1.4-nm cutoff trajectory, the Ewald technique simulation conserves the helical character of the peptide conformation. This demonstrates that even 1.4 nm is too short a cutoff. Due to the fundamental uncertainty introduced by the use of a simple cutoff, this truncation scheme seems questionable for molecular dynamics simulations of solvated biomolecules.

It is no matter of debate that the inclusion of solvent effects is essential for a realistic description of structural and dynamical features of biomolecules. From a conceptional point of view, molecular dynamics (MD) simulations taking into account explicitly solvent (usually water) molecules are the most direct way to meet this goal (Brooks et al., 1988; Karplus & Petsko, 1990; van Gunsteren & Berendsen, 1990). However, the high numerical effort has long prohibited extensive simulations of that kind.

† This work was supported by the Austrian Fonds zur Förderung der wissenschaftlichen Forschung under project number P 8472.

0006-2960/92/0431-5856$03.00/0

Due to the steadily increasing computational power, research in this direction has recently started (Berendsen et al., 1986; Levitt & Sharon, 1988; Tirado-Rives & Jorgensen, 1990). As for vacuum simulations, it is common practice to truncate Coulomb forces beyond a certain threshold r_c. As opposed to vacuum simulations, where r_c could in principle be extended to infinity (Loncharich & Brooks, 1989), toroidal boundary conditions, as applied for bulk systems, restrict r_c to values smaller than half of the box length (Allen & Tildesley, 1987). This restriction has the benefit of reducing computational effort. The usual choice for r_c falls into the range 0.8–1.0 nm. Apart from first trials (Kitson & Hagler, 1988; Kitchen et al., 1990), there are no systematic studies on the consequences of such a treatment, when solvated biomolecules are studied via molecular dynamics.

In order to elucidate this problem, we studied the response of a 17-residue model peptide, dissolved in a pool of more than a thousand water molecules, to the choice of the cutoff radius and compared the results to those of a simulation based on the Ewald summation technique (Ewald, 1921). The Ewald summation method circumvents the bad convergence properties of Coulomb interactions by splitting them into two rapidly converging series in real and reciprocal space. This technique is well established for molecular liquids and ionic melts, where it is known to model the dielectric properties of a system in the right way (Neumann & Steinhauser, 1983a; Adams & Dubey, 1987).

Model System and Methods

As a model system, we have chosen one of Baldwin's helix forming peptides (Padmanabhan et al., 1990), namely Ac-Tyr-(Lys-(Ala-)$_4$)$_3$-Lys-NH_2. Considering the non-hydrogen atoms and only the polar hydrogens, this system consists of 144 atoms. The peptide was placed into a rectangular box of dimensions $a = b = 2.9$ nm and $c = 3.9$ nm filled with 1021 water molecules and four counterions. Altogether the system is composed of 3211 atoms.

For setting up the system as well as for the simulations themselves, we have used programs of the GROMOS 86 package (van Gunsteren & Berendsen, 1987). The topology of the peptide was generated with the aid of the program PROGMT using the 37C4 version of the forcefield. After the box was filled with SPC-type water molecules according to PROBOX, PROION served to insert the respective counterions which were placed in close proximity to the lysins. All MD simulations were carried out with the program PROMD, which was augmented by special self-written subroutines for the Ewald technique. In order to eliminate high-order vibrational motions, the SHAKE algorithm (van Gunsteren & Berendsen, 1977) was applied with a time step of 2 fs. The temperature was kept near 300K by an appropriate scaling of the atomic velocities. For economic reasons, the neighborhood technique was exploited using an updating period of 10 time steps. Starting from an ideal α-helical peptide, the system was equilibrated for 150 ps during which a cutoff criterion of $r_c = 1.0$ nm was applied. The final configuration termed A further on served as the starting point for three cutoff and one Ewald simulations. A second starting configuration (B) was extracted from the 1.0–nm cutoff simulation. Thus both, A and B, lie on the same trajectory and are separated by an interval of 225 ps.

It is important to note that the cutoff criterion was based on the charge-group concept; i.e., interactions between a pair of charged groups are either kept as a whole or rejected completely depending on whether the distance between respective centers of geometry is smaller or larger than r_c.

Table I: Overview of the Simulation Runs

run no.	starting configuration	time period (ps)	treatment of nonbonded interactions
1	A	450 ps	cutoff: 0.6 nm
2	A	825 ps	cutoff: 1.0 nm
3	A	90 ps	cutoff: 1.4 nm
4	B	60 ps	cutoff: 1.4 nm
5	A	225 ps	Ewald summation

The cutoff simulations were performed on an IBM 3090/400 E at the Vienna University Computer Center, whereas the Ewald trajectory was generated on a 19-node transputer system. The technical details of the implementation will be presented in a forthcoming paper.

Results

Three independent cutoff based simulations were performed taking configuration A as a starting point. Thereby the cutoff radius r_c was systematically enlarged from $r_c = 0.6$ nm to $r_c = 1.0$ nm and finally to $r_c = 1.4$ nm, being close to the maximum value for our system compatible with toroidal boundary conditions. The three runs covered 450, 825, and 90 ps, respectively (runs 1–3 of Table I).

As the respective trajectories departed from each other very rapidly, we will concentrate on the initial 90 ps of time evolution. Figure 1 displays snapshots for all three runs taken after 30, 60, and 90 ps, respectively. Roughly speaking, the peptide loses its helical conformation in the 0.6- and 1.4-nm runs, whereas it is maintained to a considerable extent in the 1.0-nm simulation. For a more detailed analysis, we have evaluated the time evolution of the respective backbone dihedrals ϕ and ψ. Configuration A serving as a common starting point for all three cutoff simulations has ϕ and ψ values in the range from Ala-4 to Ala-15 which are close to the ideal ones, namely, −57 and −47 for ϕ and ψ, respectively.

Analyzing the 0.6-nm run first, we observe that the helix gets distorted from both the N- and the C-terminal end during the time period 0–30 ps. In particular, the ϕ angles of residue Ala-4 and Ala-15 as well as the ψ values of Ala-5 and Ala-14 depart from the ideal helix conformation. The C-terminal disorder increases in the subsequent time segment 30–60 ps (not shown graphically). In addition, a new feature emerges, namely that the ϕ and ψ values of the eighth residue, being the midpoint of the remanent helix, leave their original positions. This event initiates the final collapse of the helix observed in the 60–90-ps period. At the end only residues 2, 4, 10, and 11 have ϕ and ψ values in the vicinity of the helical ones. As there must be a minimum of three consecutive residues covering the helical area of the Ramachandran plot for the formation of a single helix turn, the 90-ps conformation lacks any helical feature.

In contrast to the 0.6-nm run the starting configuration is more or less conserved during the first 60 ps of the 1.0-nm trajectory. In the 60–90-ps period, however, there is a perturbation in the N-terminal part of the helix, while the C-terminal part is unaffected (Figure 1). In terms of backbone dihedrals, this N-terminal perturbation is reflected by $\phi_6 = -86$, $\phi_7 = -120$, and $\phi_8 = -117$ as well as $\psi_6 = 6$, $\psi_7 = 62$, and $\psi_8 = -26$ of the 90-ps snapshot.

In the 1.4-nm simulation, we observe even in the first period (0–30 ps) an enhanced mobility; i.e., the backbone dihedrals cover a broader range at least for the N-terminal half of the helix. As a result, the helix looks bent in the 30-ps snapshot of Figure 1. Subsequently, the unfolding is initiated at two sites (Ala-10 and Ala-15) in the 30–60-ps period, propagates

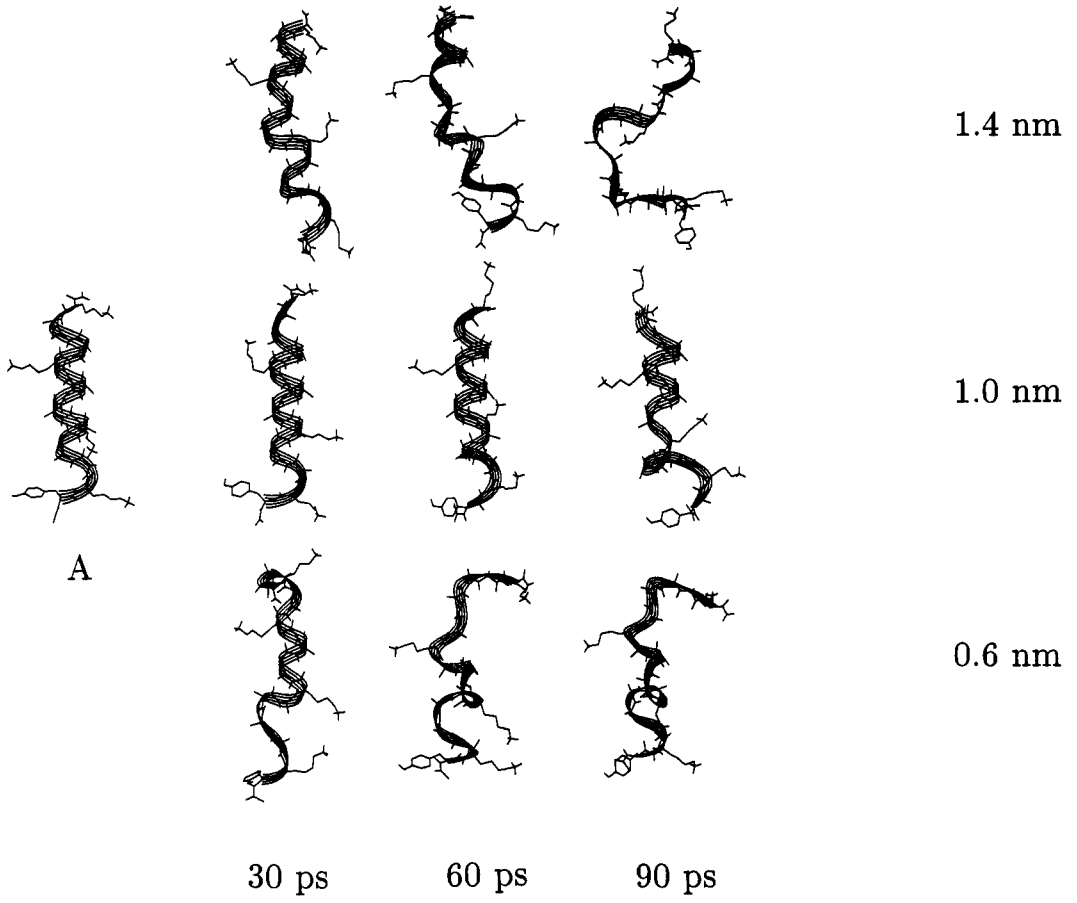

FIGURE 1: Snapshots displaying the different dynamical behavior of the model peptide Ac-Tyr-(Lys-(Ala-)$_4$)$_3$-Lys-NH$_2$ covering a time interval of 90 ps. The very left helical conformation (labeled A) is a common starting point for all three molecular dynamics runs using r_c = 1.4 nm, r_c = 1.0 nm, and r_c = 0.6 nm (top to bottom). The individual snapshots are taken at 30, 60, and 90 ps. The pictures were generated with the program INSIGHT II (Biosym, Inc.).

in the 60–90-ps time section, and finally leads to a coiled structure at 90 ps (Figure 1).

In order to test the influence of initial conditions, we have set up an additional 1.4-nm cutoff simulation starting at configuration B, which lies along the r_c = 1.0-nm trajectory and is separated from configuration A by 225 ps (run 4 of Table I). B has ideal helical dihedral angles within the range Ala-8 to Ala-14. In contrast to the typical helical hydrogen bonds between residues N and N+3, there is a hydrogen bond between Ala-4 and Ala-9, which causes a perturbed hydrogen bonding pattern because there is one excess residue in the respective helix turn. This distortion of the N-terminal part of the helix was brought about by fluctuations preceding configuration B by 135 ps (cf. the 90-ps snapshot of Figure 1, middle row). This peculiar feature is still there in the 30-ps, 60-ps, and 90-ps snapshots of the r_c = 1.0-nm simulation (see bottom of Figure 2). In other words, for the r_c = 1.0-nm simulation, the overall structure of configuration is more or less conserved within the 90 ps displayed in Figure 2.

In the first 30-ps time segment, the 1.4-nm cutoff simulation seems to maintain the overall peptide geometry of configuration B, too, but shows the same enhanced mobility already observed for the r_c = 1.4-nm simulation starting from A. However, in the subsequent 30 ps, the dihedral angles of Ala-8 to Ala-10 leave their helical positions and unfolding propagates from there to both ends (Figure 2).

As the cutoff simulations so far give no consistent picture, we have also performed a simulation based on the Ewald summation technique, in order to permit an independent judgment (run 5) (Figure 3). The result for the total 225-ps trajectory can be summarized in a single statement: all backbone dihedrals stick to values close to those they had already in configuration A, as far as the helix is concerned (Ala-4 to Ala-15). In the same time segment, the 1.0-nm cutoff simulation causes residue Ala-14 to leave the helical position at the C-terminal end and introduces the Ala-4 to Ala-9 hydrogen bond already described, because the 225-ps conformation is identical to the starting configuration B. This distortion of the N-terminal hydrogen bonding network leads to the unfolding of this part later on (data not shown) in the r_c = 1.0-nm simulation.

Discussion

In the previous section, we have learned that the stability of an α-helix is an oscillatory function of the cutoff size: For r_c = 0.6 nm the α-helix is destabilized, a fair stability is regained for 1.0 nm but is lost again for 1.4 nm and finally conserved when the Ewald technique is applied. This last point is particularly important as the Ewald summation—in some sense—may be seen as a simulation with infinite cutoff and can thus be regarded as a reference system.

It is no matter of debate that the range of cutoff radii used in this study should be appropriate for the r^{-6} tail of the Lennard–Jones potential. Therefore, it is solely to the responsibility of the Coulomb interactions to cause the different behavior of various cutoff simulations. From a mathematical point of view, it is well known that Coulomb sums represent conditionally convergent series (Glasser & Zucker, 1980). Qualitatively speaking, this means that the series seems to converge for a small number of terms but diverges when further contributions are added, and so on. In order to understand this role of the Coulomb summation, let us consider

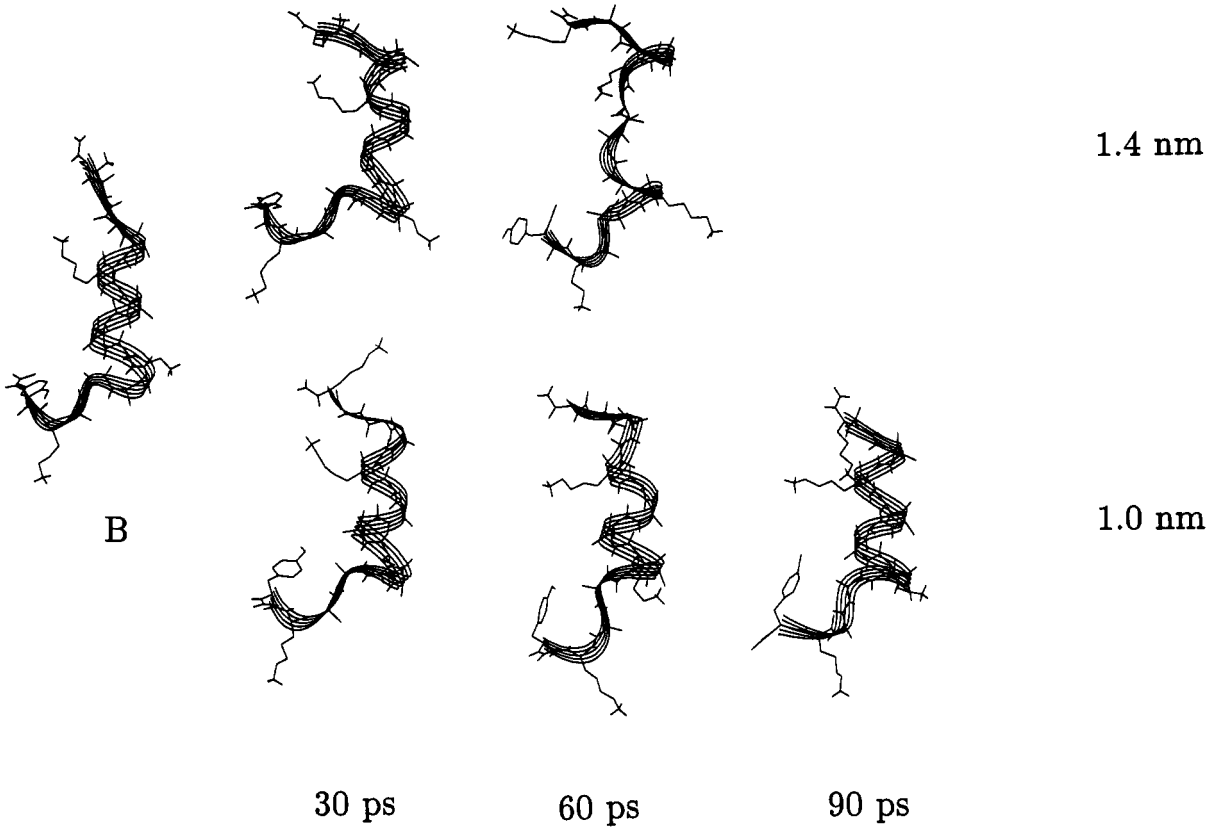

FIGURE 2: The dynamical behavior of the model peptide Ac-Tyr-(Lys-(Ala-)$_4$)$_3$-Lys-NH$_2$ displayed as a series of snapshots. In contrast to Figure 1, the common starting point for both molecular dynamics runs using r_c = 1.4 nm (top) and r_c = 1.0 nm (bottom) is now configuration B. The individual snapshots are taken at 30, 60, and 90 ps.

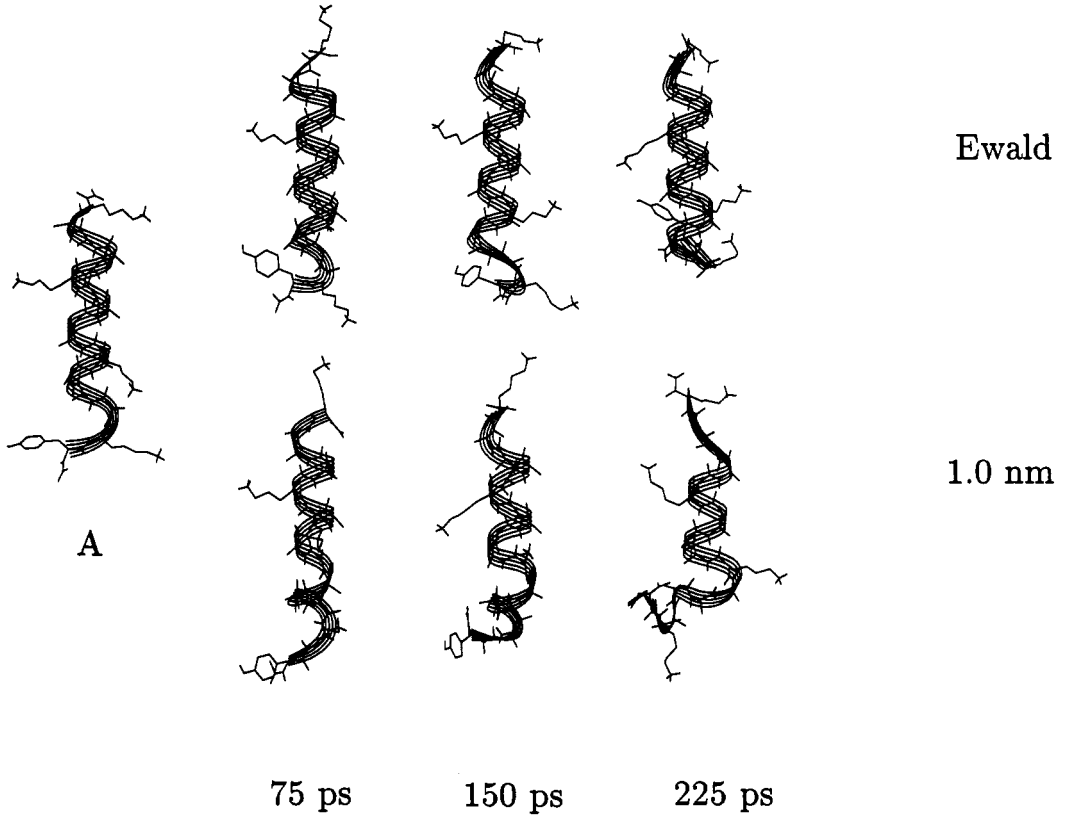

FIGURE 3: The time evolution of the model peptide Ac-Tyr-(Lys-(Ala-)$_4$)$_3$-Lys-NH$_2$ shown as a series of snapshots. As in Figure 1, the common starting point for both molecular dynamics runs using the Ewald summation technique (top) and a cutoff of r_c = 1.0 nm (bottom) is configuration A. The individual snapshots are taken at 75, 150, and 225 ps.

the neighborhood of a solute atom dissolved in a pool of water molecules: The interaction of this reference solute atom with its neighborhood may be decomposed into concentric spherical shells of increasing radius. As long as the thickness of the shells is comparable to the atomic diameters, the net charge density will change sign when going from one shell to the next

one. The interaction of the reference atom with its environment may now be viewed as a sum over the contributions from concentric shells. In addition to the fundamental dilemma that the Coulomb potential falls off with r^{-1}, whereas the number of charged particles per shell increases with r^2, the contributions from the individual shells may oscillate in sign. Therefore, the cumulative sum over the shells does not monotonously converge to the final value, but it approaches it in an oscillatory way. Due to the increasing number of particles and increasing disorder per shell, the contributions from the outer shells become weaker and weaker such that the summation finally converges.

Therefore, one cannot rule out that a specific cutoff size is fortuitously close to the correct value. This seems to be the case for our system in the r_c = 1.0-nm simulation, but it may probably be also true for other cutoffs in other systems. Due to this fundamental uncertainty and arbitrariness caused by the use of a simple cutoff criterion, we consider this procedure an inadequate means to handle long-range interactions. In this context detailed investigations of the stability and solvation of peptides (DiCapua et al., 1990, 1991; Tobias et al., 1991; Tobias & Brooks, 1991; Tirado-Rives & Jorgensen, 1991) using a simple cutoff seem to be premature.

Although the influence of various truncation schemes on the dynamic and structural properties of molecular liquids as well as ionic solutions and melts is well documented in the literature (Adams, 1979; Neumann & Steinhauser, 1983b; Neumann et al., 1984; Brooks et al., 1985; Brooks, 1987), the influence of the cutoff size on the peptide dynamics has been underestimated so far.

One might argue that a helical peptide with its high intrinsic net dipole moment is too hard a test case. Nevertheless, it is the predominant secondary structure element of proteins and must thus be treated correctly.

Finally, we want to emphasize that all arguments presented in this section refer to the correct methodic treatment within a given model, i.e., a given forcefield. It was not our intention to criticize the validity or accuracy of the model as such with respect to its capability to describe a realistic scenery.

Registry No. Ac-Tyr-[Lys-(Ala)$_4$]$_3$-Lys-NH$_2$, 135726-68-0.

References

Adams, D. J. (1979) *Chem. Phys. Lett. 62*, 329.

Adams, D. J., & Dubey G. S. (1987) *J. Comput. Phys. 72*, 156.

Allen, M. P., & Tildesly, D. J. (1987) *Computer Simulation of Liquids*, Oxford University Press, Oxford.

Berendsen, H. J. C., van Gunsteren, W. F., Zwinderman, H. R. J., & Greutsen, R. G. (1986) *Ann. N.Y. Acad. Sci. 482*, 269.

Brooks, C. L., III (1987) *J. Chem. Phys. 86*, 5156.

Brooks, C. L., III, Pettitt, B. M., & Karplus M. (1985) *J. Chem. Phys. 83*, 5897.

Brooks, C. L., III, Karplus, M., & Pettitt, B. M. (1988) *Adv. Chem. Phys. 71*, 1.

DiCapua, F. M., Swaminathan, S., & Beveridge D. L. *J. Am. Chem. Soc. 112*, 6768.

DiCapua, F. M., Swaminathan, S., & Beveridge D. L. (1991) *J. Am. Chem. Soc. 113*, 6145.

Ewald, P. (1921) *Ann. Phys.* 64, 253.

Glasser, M. L., & Zucker, I. J. (1980) in *Theoretical Chemistry: Advances and Perspectives* (Henderson, D., Ed.) Vol. 5, pp 67–138, Academic Press, New York.

Karplus, M., & Petsko, G. A. (1990) *Nature 347*, 631.

Kitchen, D. B., Hirata, F., Westbrook, J. D., Levy, R., Kofke, D., & Yarmush, M. (1990) *J. Comput. Chem. 11*, 1169.

Kitson, D. H., & Hagler, A. T. (1988) *Biochemistry 27*, 5246.

Levitt, M., & Sharon, R. (1988) *Proc. Natl. Acad. Sci. U.S.A. 85*, 7557.

Loncharich, R. J., & Brooks, B. R. (1989) *Proteins: Struct., Funct., Genet. 6*, 32.

Neumann, M., & Steinhauser, O. (1983a) *Chem. Phys. Lett. 95*, 417.

Neumann, M., & Steinhauser, O. (1983b) *Chem. Phys. Lett.* 102, 508.

Neumann, M., Steinhauser, O., & Pawley G. S. (1984) *Mol. Phys. 52*, 97.

Padmanaban, S., Marqusee, S., Ridgeway, T., Laue, T. M., & Baldwin, R. L. (1990) *Nature 344*, 268.

Tirado-Rives, J., & Jorgensen, W. L. (1990) *J. Am. Chem. Soc. 112*, 2773.

Tirado-Rives, J., & Jorgensen, W. L. (1991) *Biochemistry 30*, 3864.

Tobias, D. J., & Brooks, C. L., III (1991) *Biochemistry* 30, 6059.

Tobias, D. J., Mertz, J. E., & Brooks, C. L., III (1991) *Biochemistry 30*, 6054.

van Gunsteren, W. F., & Berendsen, H. J. C. (1977) *Mol. Phys.* 34, 1311.

van Gunsteren, W. F., & Berendsen, H. J. C. (1987) *GROningen MOlecular Simulation Library Manual*, Biomos, Groningen, The Netherlands.

van Gunsteren, W. F., & Berendsen, H. J. C. (1990) *Angew. Chem., Int. Ed. Engl. 29*, 992.